An RBF-based Artificial Neural Network for Prediction of Dynamic Viscosity of MgO/SAE 5W30 Oil Hybrid Nano-Lubricant to obtain the best performance of energy systems

Preprint *in* Materials Today Communications · December 2023

DOI: 10.1016/j.mtcomm.2023.107836

Dheyaa Jumaah Jasim
Al-Amarah University College

S.Mohammad Sajadi
Cihan University-Erbil

S. Ali Eftekhari
Islamic Azad University KhomeiniShahr

Maaboud Hekmatifar
Islamic Azad University Khomeini Shahr

Materials Today Communications xxx (xxxx) 107836

Contents lists available at ScienceDirect

Materials Today Communications

journal homepage: www.elsevier.com/locate/mtcomm

An RBF-based artificial neural network for prediction of dynamic viscosity of MgO/SAE 5W30 oil hybrid nano-lubricant to obtain the best performance of energy systems

Jie Gao [a,*], Dheyaa J. Jasim [b], S. Mohammad Sajadi [c], S. Ali Eftekhari [d,*], Maboud Hekmatifar [d], Soheil Salahshour [e,f,g], Farzad Tat Shahdost [h], Davood Toghraie [d,*]

[a] School of Engineering, Guangzhou College of Technology and Business, Guangzhou, Guangdong 510850, China
[b] Department of Petroleum Engineering, Al-Amarah University College, Maysan, Iraq
[c] Department of Nutrition, Cihan University-Erbil, Kurdistan Region, Iraq
[d] Department of Mechanical Engineering, Khomeinishahr Branch, Islamic Azad University, Khomeinishahr, Iran
[e] Faculty of Engineering and Natural Sciences, Bahcesehir University, Istanbul, Turkey
[f] Department of Computer Science and Mathematics, Lebanese American University, Beirut, Lebanon
[g] Faculty of Engineering and Natural Sciences, Istanbul Okan University, Istanbul, Turkey
[h] Electrical Control Engineering, Islamic Azad University, Garmsar Branch, Semnan, Iran

ARTICLE INFO

Keywords:
Radial Basis Function
ANN
Hybrid nanofluid
Dynamic viscosity

ABSTRACT

Technological progress and complications in microfluidics usage have led researchers to use nanomaterials in different scientific fields. The properties and characteristics of hybrid Nanofluids are more enhanced compared to nanofluids based on single nanoparticles and conventional liquid. Recently, modeling methods have replaced most common statistical methods. Due to the high accuracy of the response and generalizability in various conditions, artificial neural networks (ANNs) to estimate nanofluids' viscosity and thermal conductivity have become common. Dynamic viscosity (μ) (estimation analyzes one of the key factors in determining the hydrodynamic behavior of nanofluids. In this manuscript, an RBF-ANN is used to simulate the input-output relation of dynamic viscosity of the MgO- SAE 5W30 Oil hybrid nanofluid versus three important parameters, including volume fraction of nanoparticles, temperature, and shear rate. The results show that for this nanofluid, by increasing temperature and shear rate, the dynamic viscosity is decreased. In contrast, the volume fraction of nanoparticles directly affects the output, although this consequence can be neglected. By increasing the temperature from 5° to 55°C, the dynamic viscosity would decrease. Also, changing the shear rate from 50 to 1000 rpm decreases the dynamic viscosity from 400 cP to 25 cP. It is worth mentioning that the obtained trends and deviation of dynamic viscosity for MgO-SAE 5W30 Oil hybrid nanofluid versus temperature, the volume fraction of nanoparticles, and shear rate can be used by the academic community as well as an industrial section to obtain the best performance of energy systems based on this nanofluid.

Nomenclature

A_i	RBF neurons of hidden layer.
p	Input vector.
R^2	R-square.
T	Temperature (C).
w	Weight vector.
x	n dimensional input vector.
y	Target values.
$\hat{y}$	True outputs of the RBF network.
$\|\cdot\|$	Norm.
μ	Radial function center.
ϕ	Nanoparticle fraction/Radial basis function.

* Corresponding authors.
E-mail addresses: gaojiestudy@163.com (J. Gao), s.a.eftekhari@iaukhsh.ac.ir (S.A. Eftekhari), toghraee@iaukhsh.ac.ir (D. Toghraie).

https://doi.org/10.1016/j.mtcomm.2023.107836
Received 15 October 2023; Received in revised form 5 December 2023; Accepted 8 December 2023
2352-4928/

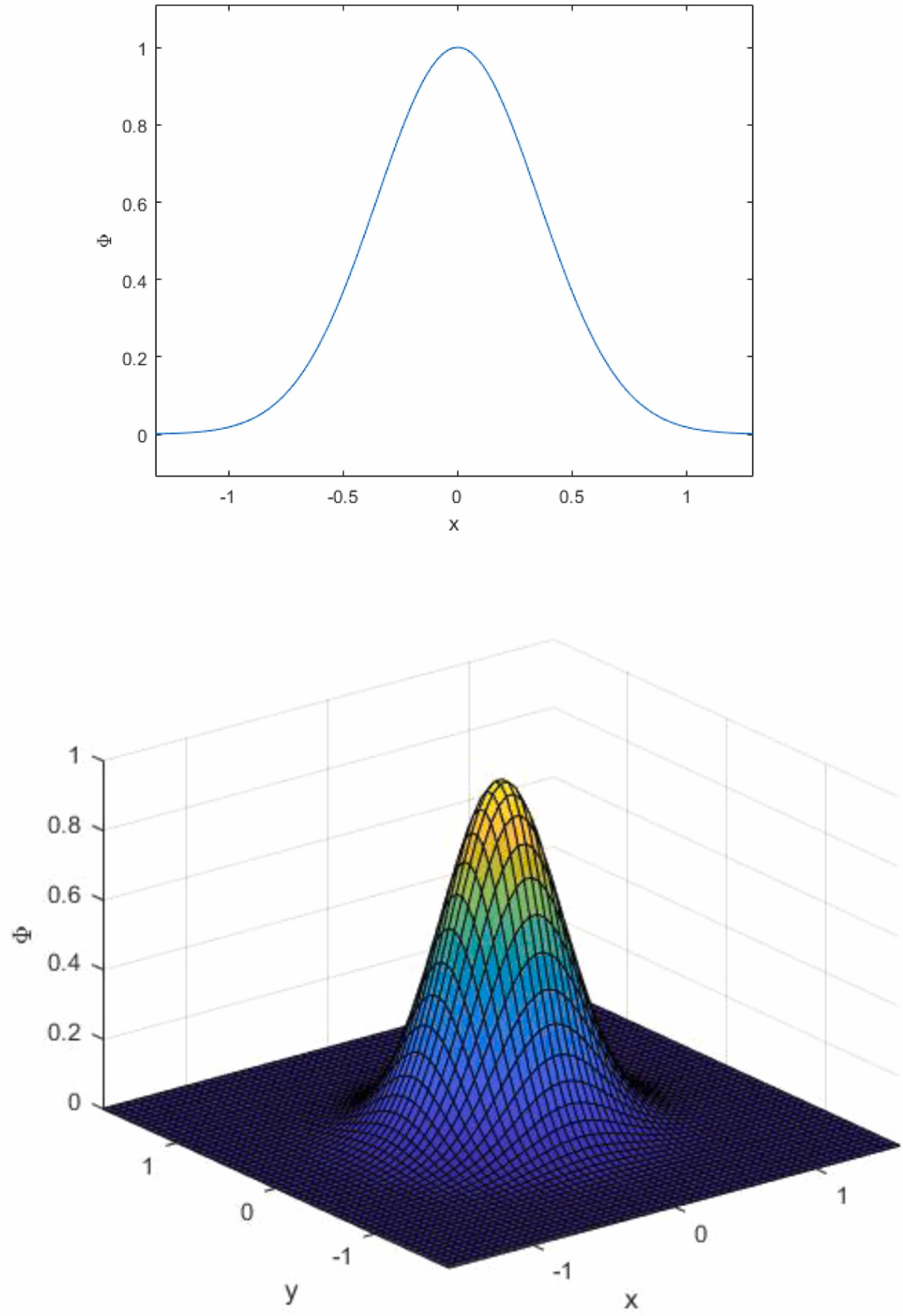

Fig. 1. Gaussian RBF in 2D and 3D space.

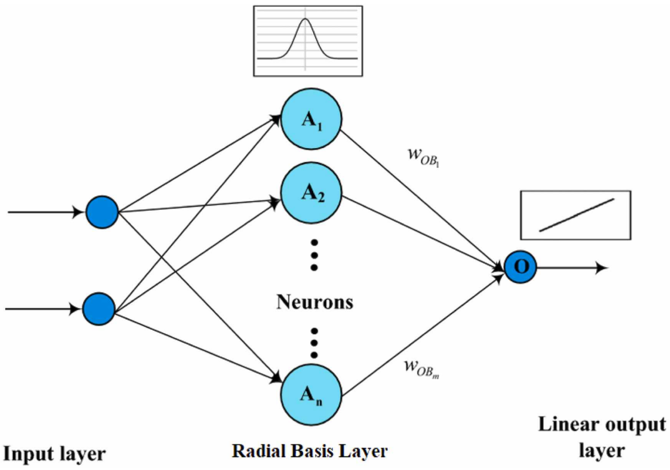

Fig. 2. A schematic representation of the Radial Basis Neuron.

1. Introduction

Technological progress and the occurrence of complications in microfluidics usage, including equipment damage, sedimentation in ducts, extreme fluid pressure drop, and improper particle suspension in fluid, have led researchers to use Nanomaterial in different scientific fields [1]. Recent studies on nanofluids have introduced an advanced fluid classification with enhanced thermal properties called hybrid nanofluids, obtained by dispersing nanocomposites or nanoparticles of various metals in a base fluid such as water, ethylene glycol, or oil [2]. Hybrid nanofluids' properties and characteristics are more enhanced than nanofluids based on single nanoparticles and conventional liquids [3]. Researchers have proven that metal oxide particles such as CuO, MgO, and TiO_2 have an effective role in improving the properties of nanofluids due to their high elastic modulus, oxidation resistance, corrosion resistance, and high temperature tolerance [4]. Hemmat Esfe et al. [5] investigated the effects of increasing temperature and concentration of copper and titanium oxide nanoparticles in the various temperature ranges of 65–95 °C and up to a volume fraction of 2%. The fluid was also a hybrid and a mixture of water and ethylene glycol. This study showed an increase in the thermal conductivity to 44% at 65 °C and the volume fraction to 2%. Vafaie et al. [6] also investigated the effect of hybrid nanoparticles of carbon nanotubes and MgO on the thermal conductivity of ethylene glycol. This study shows that by increasing the number of nanoparticles and increasing the temperature, the thermal conductivity increases by 29%.

Recently, modeling methods have replaced most common statistical methods due to their high efficiency, reliability, and flexibility. Due to the high accuracy of the response and generalizability in various conditions, the use of ANNs to estimate the viscosity and thermal conductivity of nanofluids has become common [7]. The results showed that the ANN with this training algorithm could predict the Nusselt number with high accuracy. Also, in terms of calculation time, this method calculates the results quickly. For example, Tian et al. [8] investigated the influence of temperature and volume fraction of nanoparticles on the thermal conductivity of Graphene oxide-Al_2O_3/Water-Ethylene glycol hybrid nanofluid. The results showed that ANN was well trained using the trainbr algorithm and had a correlation coefficient of 0.999 for thermal conductivity. Finally, the results showed that increasing the nanofluid temperature has less effect on improving the thermal conductivity than the volume fraction of nanoparticles. Hemmat Esfe et al. [9] investigated the thermal conductivity of MgO/ethylene glycol (EG) nanofluids in the temperature range of 25–55 °C and a volume concentration of up to 5%. It has been observed that the neural network can be used as a powerful tool to predict the thermal conductivity of nanofluids.

One of the most important properties of nanofluid is dynamic viscosity, that affects the flow and pumping power of the fluid and its thermal behavior. In most cases, the viscosity of the nanofluid is higher than that of the base fluid. Viscosity estimation analyses are key factors in determining the hydrodynamic behavior of nanofluids [10]. Nanofluid viscosity depends on temperature, particle size, nanoparticle volume fraction, and shear rate [11]. The obtained results from the study of dynamic viscosity of MWCNT-carbon/SAE 10 W40-SAE 85W90 showed that the effect of temperature on dynamic viscosity is dominant compared to the shear rate and concentration. In this study, the temperature and concentration of nanoparticles were defined as the input of the ANN. The recommended R^2 value of ANN was 1, which showed good performance in predicting dynamic viscosity [12]. The results of the researchers showed that another factor influencing the dynamic viscosity is the shear rate. In some models, this parameter was considered as an input variable. For example, Toghraie et al. [13] considered temperature, shear rate, and concentration as inputs and influential factors for predicting the dynamic viscosity of Tungsten Oxide (WO_3)-MWCNTs/Engine Oil hybrid nanofluid in the ANN model. The R^2 value of the ANN model in this study was 0.9948, which indicates the accuracy and good performance of the model. Hemmat et al. [14] predicted the dynamic viscosity of Al_2O_3-engine oil nanofluid using an ANN. Their results showed that the use of ANN leads to better results. Using the RBF-ANN model, the effect of volume percentage and temperature on the viscosity of Al_2O_3/Water nanofluid was investigated, which is well consistent with experimental data [15].

A review of previous research has shown that no research was conducted on a hybrid nanofluid consisting of SAE5W30 as the base fluid and MgO. Also, due to the complex mechanism and structure of nanofluids, in this study, the data obtained from the viscosity of the nanofluid are simulated with artificial RBF ANNs. In addition, the effects of volume fraction, temperature, and shear rate on the viscosity of the hybrid nanofluid are investigated. Finally, an attempt will be made to propose an optimal model to evaluate the dynamic viscosity of this nanofluid.

2. Radial basis function network

Recently, modeling using machine learning and artificial intelligence methods have replaced most common statistical methods due to their high efficiency, reliability, and flexibility [18–23]. Artificial Neural Networks (ANNs) are currently the most widely used Machine

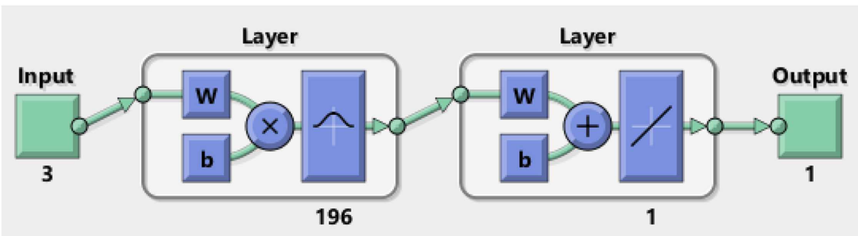

Fig. 3. RBF–ANN created for simulation of dynamic viscosity of hybrid nanofluid versus input parameters.

Table 1
Dynamic viscosity of MgO-SAE 5W30 Oil hybrid nanofluid samples used for training the RBF ANN.

ϕ (%)	T (°C)	Shear Rate (rpm)	μ (cP)	ϕ (%)	T (°C)	Shear Rate (rpm)	μ (cP)	ϕ (%)	T (°C)	Shear Rate (rpm)	μ (cP)	ϕ (%)	T (°C)	Shear Rate (rpm)	μ (cP)
1.5	5	50	428	1	45	500	49.1	0.5	25	600	106.6	0.1	15	400	163.6
1.5	5	100	399	1	45	600	47.5	0.5	35	300	71.9	0.1	15	500	160.1
1.5	5	200	387.2	1	45	700	46.3	0.5	35	400	70.3	0.1	15	600	156.9
1.5	5	300	374.4	1	45	800	46.2	0.5	35	500	69	0.1	25	200	104.1
1.5	15	100	227	1	55	600	30.9	0.5	35	600	69.4	0.1	25	300	101.9
1.5	15	200	212.8	1	55	700	29.2	0.5	35	700	69.1	0.1	25	400	98.9
1.5	15	300	208.1	1	55	800	32.6	0.5	45	400	47.3	0.1	25	500	97.1
1.5	15	400	203	1	55	900	28.5	0.5	45	500	47.6	0.1	25	600	95
1.5	15	500	198.4	0.75	5	50	401	0.5	45	600	45.6	0.1	35	300	65.6
1.5	25	200	127.5	0.75	5	100	384	0.5	45	700	44.5	0.1	35	400	62.8
1.5	25	300	123.7	0.75	5	200	358.1	0.5	45	800	44.5	0.1	35	500	61.5
1.5	25	400	120.9	0.75	5	300	350	0.5	55	700	27.9	0.1	35	600	60
1.5	25	500	118.5	0.75	15	100	216	0.5	55	800	30.7	0.1	35	700	58.7
1.5	25	600	116.3	0.75	15	200	208.1	0.5	55	900	27.3	0.1	45	500	40.9
1.5	35	300	78.1	0.75	15	300	199.4	0.5	55	1000	26.1	0.1	45	600	38.8
1.5	35	400	76.4	0.75	15	400	194.1	0.25	5	100	354	0.1	45	700	37.5
1.5	35	500	74.6	0.75	15	500	188.6	0.25	5	200	336.6	0.1	45	800	38
1.5	35	600	73.4	0.75	25	200	124.7	0.25	5	300	323.1	0.1	45	900	36
1.5	35	700	72.1	0.75	25	300	120.6	0.25	5	400	313.1	0.1	55	800	26.3
1.5	45	400	50.6	0.75	25	400	117.7	0.25	15	100	203	0.1	55	900	21.7
1.5	45	500	49.1	0.75	25	500	114.8	0.25	15	200	191.3	0.1	55	1000	20.4
1.5	45	600	48.1	0.75	25	600	111.9	0.25	15	300	184.4	0.0625	5	100	497
1.5	45	700	46.9	0.75	35	300	76.9	0.25	15	400	179.1	0.0625	5	200	477.2
1.5	45	800	46.6	0.75	35	400	73.6	0.25	15	500	174.7	0.0625	5	300	461.2
1.5	55	600	31.9	0.75	35	500	72.4	0.25	25	200	117.2	0.0625	15	100	358
1.5	55	700	29.5	0.75	35	600	70.3	0.25	25	300	111.9	0.0625	15	200	345
1.5	55	800	31.6	0.75	35	700	69.4	0.25	25	400	107.8	0.0625	15	300	335.6
1.5	55	900	29	0.75	45	400	47.8	0.25	25	500	105	0.0625	30	400	327.7
1.5	55	1000	28.7	0.75	45	500	48	0.25	25	600	103.1	0.0625	30	500	321.4
1	5	50	413	0.75	45	600	45.6	0.25	35	300	70.6	0.0625	35	100	272
1	5	100	388	0.75	45	700	44.7	0.25	35	400	68.4	0.0625	35	200	261.6
1	5	200	372.2	0.75	45	800	45	0.25	35	500	67.1	0.0625	35	300	255.6
1	5	300	361.9	0.75	55	700	28.4	0.25	35	600	65.3	0.0625	35	400	250.3
1	15	100	219	0.75	55	800	30.7	0.25	35	700	64	0.0625	35	500	246
1	15	200	209	0.75	55	900	27.5	0.25	45	500	45.4	0.0625	40	100	203
1	15	300	203.1	0.75	55	1000	26.4	0.25	45	600	43.1	0.0625	40	200	196.9
1	15	400	197.8	0.5	5	50	386	0.25	45	700	41.3	0.0625	40	300	193.1
1	15	500	193.9	0.5	5	100	364	0.25	45	800	42	0.0625	40	400	189.8
1	25	200	125.6	0.5	5	200	345.9	0.25	45	900	40.6	0.0625	40	500	186
1	25	300	121.3	0.5	5	300	331.9	0.25	55	700	26.2	0.0625	45	200	150.9
1	25	400	119.5	0.5	15	100	208	0.25	55	800	28.6	0.0625	45	300	148.1
1	25	500	116.3	0.5	15	200	195	0.25	55	900	25.8	0.0625	45	400	145.3
1	25	600	114.1	0.5	15	300	188.8	0.25	55	1000	25.1	0.0625	45	500	143.6
1	35	300	76.3	0.5	15	400	183.3	0.1	5	100	322	0.0625	45	600	141.3
1	35	400	75.5	0.5	15	500	179.2	0.1	5	200	305.6	0.0625	50	200	117.2
1	35	500	73.5	0.5	25	200	118.1	0.1	5	300	294.4	0.0625	50	300	114.4
1	35	600	72.2	0.5	25	300	113.7	0.1	5	400	286.4	0.0625	50	400	113
1	35	700	71.3	0.5	25	400	110.6	0.1	15	200	173.4	0.0625	50	500	111
1	45	400	48.8	0.5	25	500	108.4	0.1	15	300	168.1	0.0625	50	600	109.7

Table 2
RBF network information.

	Network parameters/ functions	Value/function
Network dimension	Number of inputs	1 cell containing 3 parameters
	Number of Layers	2
	Number of Outputs	1
	Number of Weights	981
Functions	Initialization function	initlay
	Performance Function	MSE
	Showing the Network	view
	Simulation Network	sim
	computing Performance	perform

Learning techniques which are used in different applications [24–28]. Radial basis ANNs consist of a vast number of radial basis functions [29, 30]. There are two variants of radial basis networks: generalized regression networks (GRNN) and probabilistic ANNs (PNN) [16]. In general, a radial basis can be presented by the following function:

$$z(x) = \phi(\|x - \mu\|) \tag{1}$$

where x is an n-dimensional vector that shows the center of radial basis functions. Also, ||.|| describes the Euclidian norm and is defined for positive input values refer to profile function. Usually, an RBF network consists of many (N) radial basis functions combined linearly with N distinct and various centers. Assuming x as an input, the RBF-ANN output would be the activity vector shown below:

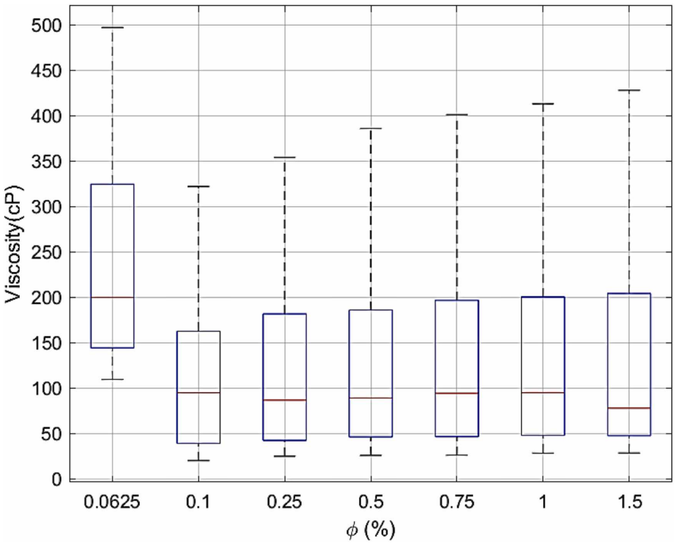

Fig. 4. Dynamic viscosity deviation versus volume fraction of nanoparticles.

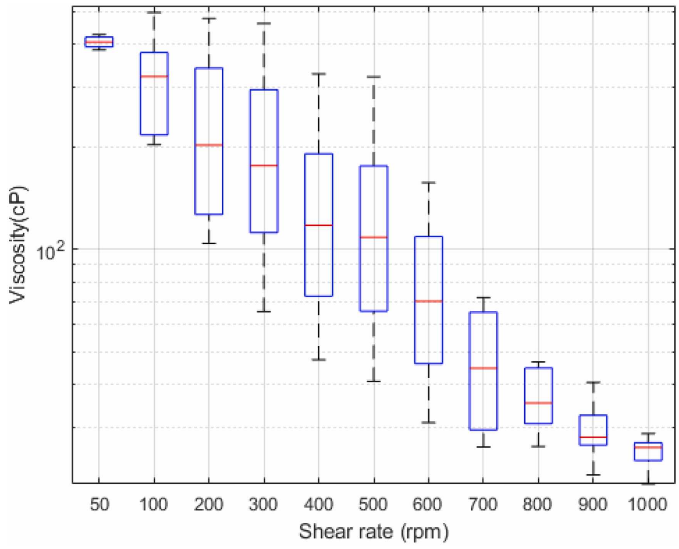

Fig. 6. Dynamic viscosity deviation versus shear rate.

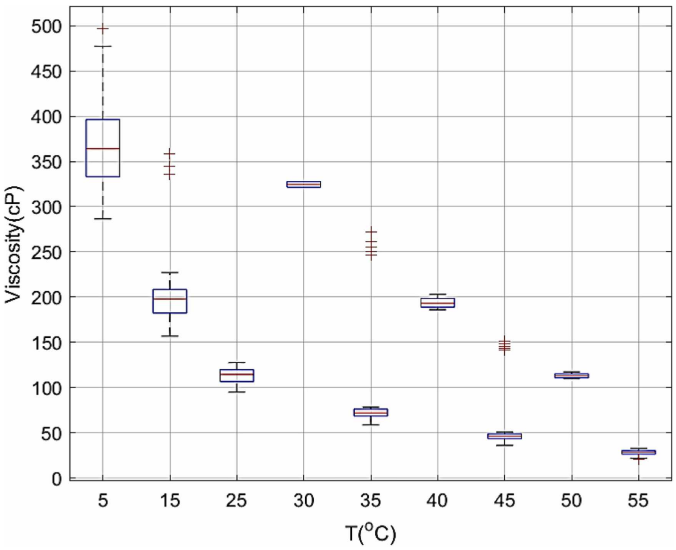

Fig. 5. Dynamic viscosity deviation versus temperature.

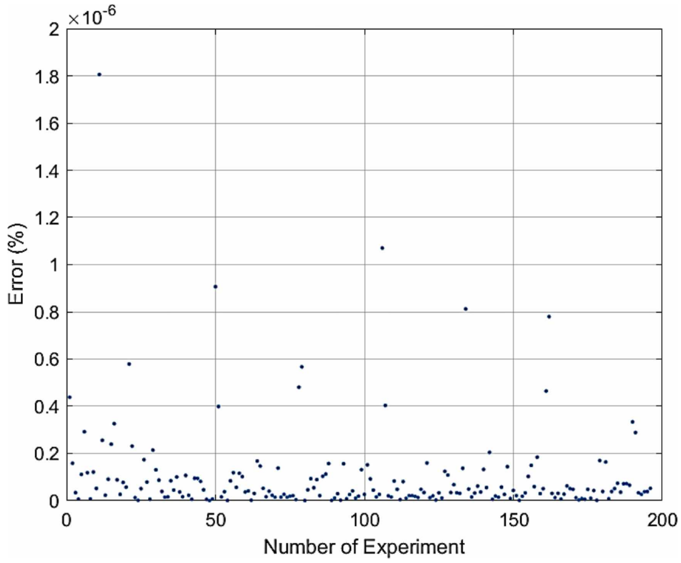

Fig. 7. Error plot of RBF network outputs.

$$\widehat{y}(x) = z\sum_{j=1}^{N}\beta_j z_j(x) \tag{2}$$

In the above relation, the weight of the jth RBF with the center of $\mu_j$and z_j is defined in the first equation. $\widehat{y}(x)$ is the true output approximating the target values denoted by y. Radial basis functions are available in various forms of functions, each of them characterized by the form of ϕ. These functions are associated with σ defining the spread of the function ϕ around the center called the width parameter. The most commonly used profile function for regression using ANNs is the Gaussian function presented as follows:

$$\phi(r) = e^{\left(-\frac{r^2}{\sigma^2}\right)} \tag{3}$$

Hence, the related RBF would be as

$$z(x) = e^{\left(\frac{\|x-\mu\|^2}{\sigma^2}\right)} \tag{4}$$

In this relation, the width parameter is assumed to be the same as the standard deviation of the Gaussian function. A schematic of Gaussian RBF is depicted in 2D and 3D in Fig. 1a and b, respectively.

An RBF outputs a maximum of 1 for 0 input; hence, the output increases by decreasing the distance of *w* and *p*. An RBF can be assumed as a detector producing 1 for identical input *p* and weight vector *w*. An RBF neuron is shown in Fig. 2.

Using several neurons in the hidden layer creates an RBF-ANN configured like Fig. 3.

In this configuration, A_i is the radial basis neuron in the hidden layer, and *O* represents the output neuron having a linear activation function. There is two variant of functions in MATLAB for the creation of RBF-ANN. The exact design is done using the function *newrbe,* and the more efficient design is attained using *newrb*. The first function creates ANNs with zero error by adding neurons in the hidden layer, while the latter function uses a Goal value for implementing a much lower number of neurons in the hidden layer. Here may raise a question: why not always use an RBF network instead of a feed-forward network? To answer this question, we should note that RBF networks, even in the efficient version, usually tend to have much more neurons than a similar

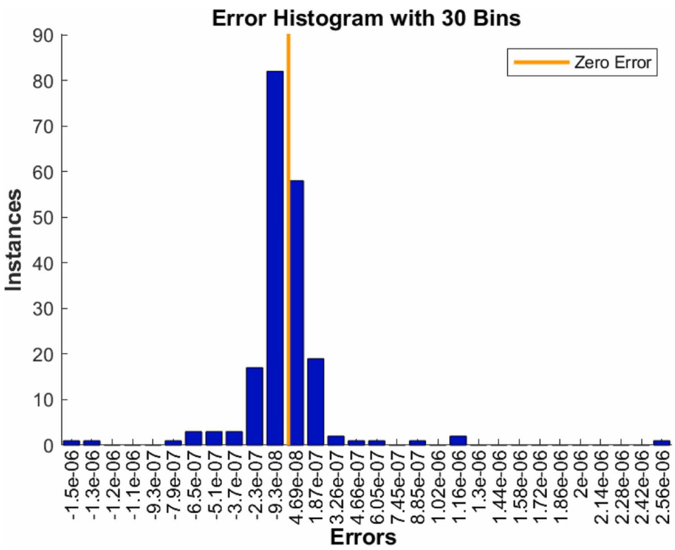

Fig. 8. Error histogram for RBF network.

feed-forward network in their hidden layers. That is because neurons in feed-forward networks, due to sigmoid functions, have outputs over a wide range of input parameters.

In contrast, RBF neurons have a small region of input parameters because of the intrinsic shape of the Gaussian function. On the other hand, the RBFs usually consume much less time for the training phase than feed-forward networks. Therefore, although these networks require more neurons than standard feed-forward back-propagation networks, they are often designed less, especially when there are many training vectors. For learning the RBF network, a dataset is needed to feed the network as different samples. The data used in this context consists of three inputs (including nanoparticle volume fraction in 7 levels from 0.0625% to 0.5%, temperature in 9 levels from 5° to 55°C, and shear rate in eleven levels from 50 to 1000 rpm) and one output (Dynamic viscosity). These data are gathered in Table 1. A total of 196 different combinations of three input parameters were examined, and the dynamic viscosity was computed. In contrast to feed-forward ANNs, the training algorithm is iterative; the learning of an RBF network is almost straightforward and successively done by adding RBF neurons to reach a predefined error. Hence, in this case, all data are used for training, while in feed-forward networks, data is divided into three categories.

In the exact version of the RBF network, the algorithm will create neurons the same number as input samples with input weight values equal to three inputs of samples. The only task for obtaining outputs close to targets is tuning the output layer weights.

3. RBF network training procedure

The training process of an RBF network has consisted of the following steps:

- **Data Preprocessing:** The input data was preprocessed by normalizing the features to ensure consistent ranges. We used MATLAB's built-in function, normalize, to perform this step.
- **Selecting RBF Centers:** To determine the centers for the RBF neurons, the K-means clustering algorithm available in MATLAB's Statistics and Machine Learning Toolbox is used.
- **Computing RBF Activations:** the activation values of each RBF neuron are computed using a Gaussian function. The distance between the input data and the centers was calculated using MATLAB's *pdist2* (Eq. 3).
- **Solve for Network Weights:** MATLAB's pinv function (pseudo-inverse) is utilized to solve the system of linear equations and determine the weights that adjust the RBF neuron outputs.
- **Test and Validate:** We evaluated the trained RBF network's performance on a separate validation dataset. We measured regression error using *mse* and *perform* metric by MATLAB built in function.

4. Results and discussion

After training, the performance of the network can be computed using the function of *perform*. The main information of created network is summarized in Table 2.

To better understand the deviation of dynamic viscosity versus each input parameter, boxplots of dynamic viscosity are depicted versus each input parameter in Figs. 4–6.

Looking above figures, several points can be drawn. First of all, the volume fraction of nanoparticles directly affects the output, while the temperature and shear rate have an inverse influence on dynamic viscosity. Moreover, the range of deviation of dynamic viscosity due to volume fraction variation of nanoparticles is much lower than the other two parameters. The decrease of viscosity with increase of temperature and shear rate can be explained as follows: With increasing temperature, the enhanced particle motion causes a reduction in particle-particle interactions and collisions, resulting in decreased viscosity. The shear rate determines the rate at which the nanofluid flows or experiences deformation under applied shear stress. When the shear rate is increased, it creates a stronger shear force on the nanofluid, leading to the rearrangement and alignment of nanofluid particles. In the case of nanofluids, the presence of nanoparticles affects the flow properties. With the application of higher shear rates, the nanoparticles reorient and align themselves in the direction of flow, reducing resistance and enhancing flowability. This realignment and directional arrangement of particles result in a decrease in dynamic viscosity.

Before checking the results of the RBF network, we should check its performance. To this end, the error plot and its histogram are investigated in Figs. 7 and 8.

According to the above figures, the trained RBF network has good performance because the outputs coincide with target values. Therefore, the created network can predict the dynamic viscosity of MgO-SAE 5W30 Oil hybrid nanofluid with almost zero error. Figs. 9–11.

5. Conclusion

In this manuscript, an RBF ANN is used to simulate the input-output relation of dynamic viscosity of the MgO- SAE 5W30 Oil hybrid nanofluid versus three important parameters, including volume fraction of nanoparticles, temperature, and shear rate. The range of parameters is as follows: in 7 levels, 9 levels, and 11 levels. By combining the above values for the input parameters, 196 samples were obtained and for each case, the dynamic viscosity is examined and computed. Then an RBF-ANN is fitted on the attained data to model the input-output dependency. The results for network output are compared to the targets, and various indices like MSE and histogram are checked to assess the appropriateness of the trained RBF network. The MSE value for this case is 1.04e-13, which shows the correctness of the RBF network. Also, the other figures show the goodness of obtained network, and its results can be used for further studies like optimization of dynamic viscosity for this network. The main results of this study can be noted as follows according to different simulations and network optimizations:

- According to obtained graphs and results, the trained network can provide dynamic viscosity prediction for MgO-SAE 5W30 Oil hybrid nanofluid versus three input parameters in the aforementioned margins.

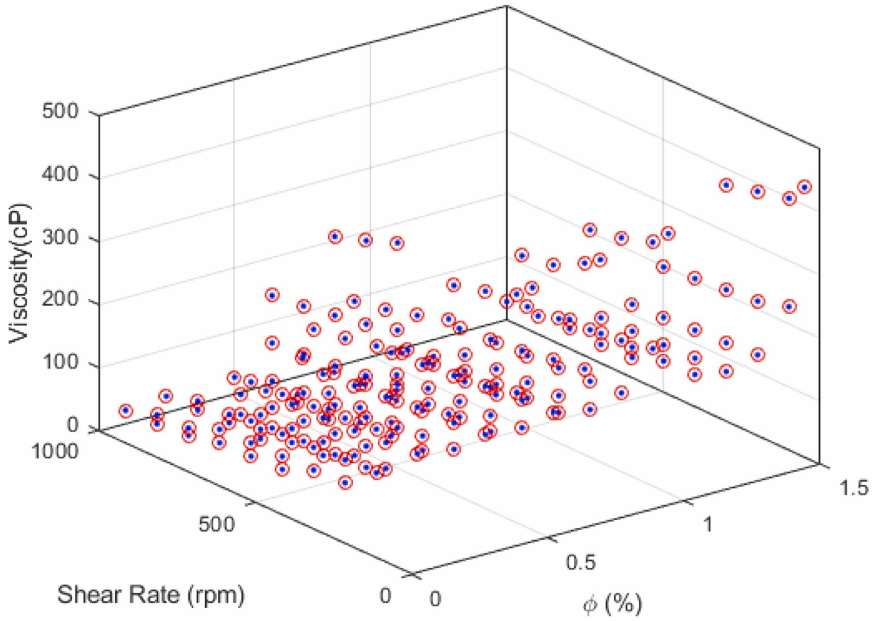

Fig. 9. Comparison of RBF network output and targets versus volume fraction of nanoparticles and shear rate.

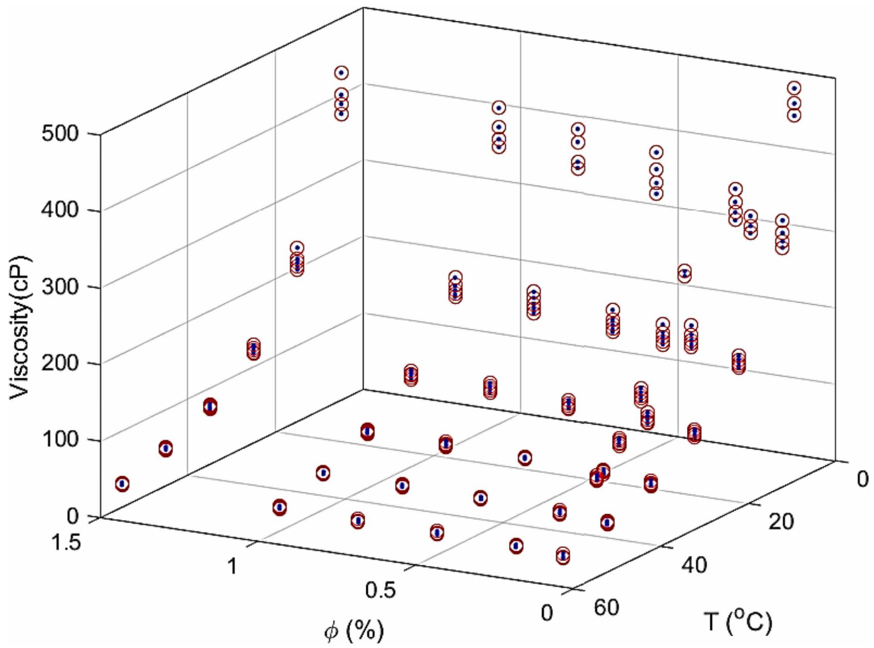

Fig. 10. Comparison of RBF network output and targets versus volume fraction of nanoparticles and temperature.

- For this nanofluid, the temperature and shear rate have the highest influence on dynamic viscosity. On the other hand, the volume fraction of nanofluid is almost effectless.
- The influence of temperature and shear rate is inverse, and by increasing these parameters, the dynamic viscosity would be decreased. In contrast, the volume fraction of nanoparticles directly affects the output, although this consequence can be neglected.
- To be more precise, by increasing the temperature from 5 to 55 degrees centigrade, the dynamic viscosity would decrease from 375 cP to around 25 cP.
- Also, changing the shear rate from 50 to 1000 will level down the dynamic viscosity from 400 cP to 25 cP.

It is worth mentioning that the obtained trends and deviation of dynamic viscosity for MgO- SAE 5W30 Oil hybrid nanofluid versus temperature, the volume fraction of nanoparticles, and shear rate may be used by the academic community as well as an industrial section to obtain the best performance of energy systems based on this nanofluid.

Uncited reference

[17].

Edit Preview PDF

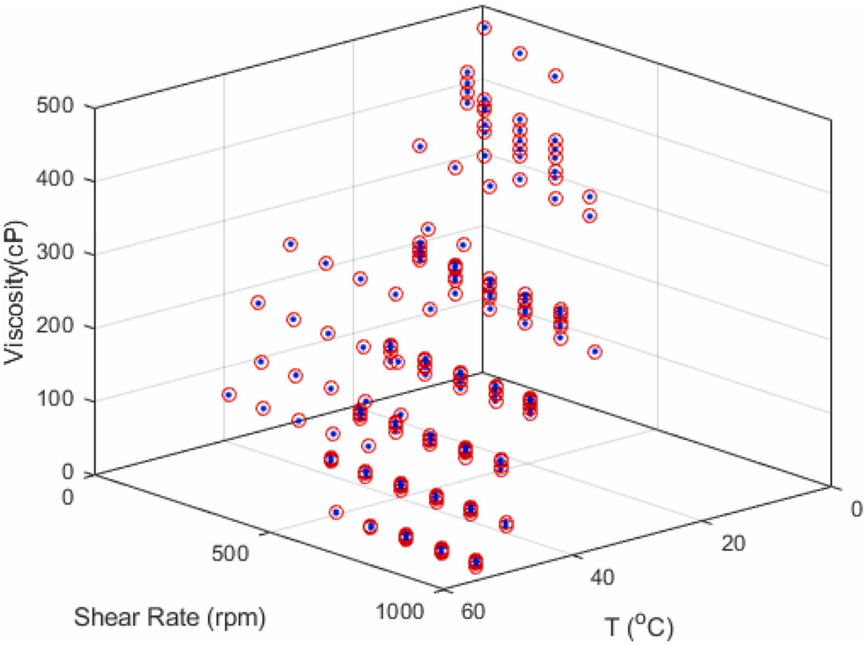

Fig. 11. Comparison of RBF network output and targets versus temperature and shear rate.

Declaration of Competing Interest

The authors declare that they have no known competing financial interests or personal relationships that could have appeared to influence the work reported in this paper.

Data Availability

No data was used for the research described in the article.

References

[1] B. Bakthavatchalam, K. Habib, R. Saidur, B.B. Saha, K. Irshad, Comprehensive study on nanofluid and ionanofluid for heat transfer enhancement: a review on current and future perspective, J. Mol. Liq. vol. 305 (2020) 112787.

[2] Y. Li, S. Tung, E. Schneider, S. Xi, A review on development of nanofluid preparation and characterization, Powder Technol. vol. 196 (2) (2009) 89–101.

[3] N.A.C. Sidik, I.M. Adamu, M.M. Jamil, G. Kefayati, R. Mamat, G. Najafi, Recent progress on hybrid nanofluids in heat transfer applications: a comprehensive review, Int. Commun. Heat. Mass Transf. vol. 78 (2016) 68–79.

[4] H.W. Xian, N.A.C. Sidik, S.R. Aid, T.L. Ken, Y. Asako, Review on preparation techniques, properties and performance of hybrid nanofluid in recent engineering applications, J. Adv. Res. Fluid Mech. Therm. Sci. vol. 45 (1) (2018) 1–13.

[5] M.H. Esfe, S. Wongwises, A. Naderi, A. Asadi, M.R. Safaei, H. Rostamian, M. Dahari, A. Karimipour, Thermal conductivity of Cu/TiO_2–water/EG hybrid nanofluid: experimental data and modeling using artificial neural network and correlation, Int. Commun. Heat. Mass Transf. vol. 66 (2015) 100–104.

[6] M. Vafaie, M. Afrand, An experimental investigation on effect of hybrid solid MWCNTs and MgO on thermal conductivity of ethylene glycol, J. Simul. Anal. Nov. Technol. Mech. Eng. vol. 9 (3) (2016) 431–440.

[7] M. Ramezanizadeh, M.H. Ahmadi, M.A. Nazari, M. Sadeghzadeh, L. Chen, A review on the utilized machine learning approaches for modeling the dynamic viscosity of nanofluids, Renew. Sustain. Energy Rev. vol. 114 (2019) 109345.

[8] S. Tian, N.I. Arshad, D. Toghraie, S.A. Eftekhari, M. Hekmatifar, Using perceptron feed-forward Artificial Neural Network (ANN) for predicting the thermal conductivity of graphene oxide-Al_2O_3/water-ethylene glycol hybrid nanofluid, Case Stud. Therm. Eng. vol. 26 (2021) 101055.

[9] M.H. Esfe, S. Saedodin, M. Bahiraei, D. Toghraie, O. Mahian, S. Wongwises, Thermal conductivity modeling of MgO/EG nanofluids using experimental data and artificial neural network, J. Therm. Anal. Calorim. vol. 118 (1) (2014) 287–294.

[10] W. Safiei, M.M. Rahman, R. Kulkarni, M.N. Ariffin, Z.A. Abd Malek, Thermal conductivity and dynamic viscosity of nanofluids: a review, J. Adv. Res. Fluid Mech. Therm. Sci. vol. 74 (2) (2020) 66–84.

[11] M.H. Esfe, S. Saedodin, S. Wongwises, D. Toghraie, An experimental study on the effect of diameter on thermal conductivity and dynamic viscosity of Fe/water nanofluids, J. Therm. Anal. Calorim. vol. 119 (3) (2015) 1817–1824.

[12] H. Maddah, R. Aghayari, M. Mirzaee, M.H. Ahmadi, M. Sadeghzadeh, A.J. Chamkha, Factorial experimental design for the thermal performance of a double pipe heat exchanger using Al_2O_3-TiO_2 hybrid nanofluid, Int. Commun. Heat. Mass Transf. vol. 97 (2018) 92–102.

[13] D.S. Toghraie, N. Sina, M. Mozafarifard, A. a Alizadeh, F. Soltani, M.A. Fazilati, Prediction of dynamic viscosity of a new non-Newtonian hybrid nanofluid using experimental and artificial neural network (ANN) methods, Heat. Transf. Res. vol. 51 (15) (2020).

[14] M. Hemmat Esfe, D. Toghraie, An optimal feed-forward artificial neural network model and a new empirical correlation for prediction of the relative viscosity of Al_2O_3-engine oil nanofluid, Sci. Rep. vol. 11 (1) (2021) 1–14.

[15] F. Derakhshanfard, A. Mehralizadeh, Application of artificial neural networks for viscosity of crude oil-based nanofluids containing oxides nanoparticles, J. Pet. Sci. Eng. vol. 168 (2018) 263–272.

[16] C. Cowan, P. Grant, S. Chen, Orthogonal least squares learning algorithm for radial basis function networks, IEEE Trans. Neural Netw. vol. 2 (2) (1991) 302–309.

[17] F.D. Foresee, M.T. Hagan, "Gauss-Newton approximation to Bayesian learning." pp. 1930–1935.

[18] B.K. Liu, W.Z. Lu, Surrogate models in machine learning for computational stochastic multi-scale modelling in composite materials design, Int. J. Hydromechatronics Vol. 5 (No. 4) (2022) 336–365.

[19] H. Gaur, B. Khidhir, R.K. Manchiryal, Solution of structural mechanic's problems by machine learning, Int. J. Hydromechatronics Vol. 5 (No. 1) (2022) 22–43.

[20] C. Hebbi, Mamatha H.R, Comprehensive dataset building and recognition of isolated handwritten kannada characters using machine learning models, Artif. Intell. Appl. (2023), https://doi.org/10.47852/bonviewAIA3202624.

[21] Guo, Y., Mustafaoglu, Z., Koundal, D. , 2022. Spam Detection Using Bidirectional Transformers and Machine Learning Classifier Algorithms. Journal of Computational and Cognitive Engineering. https://doi.org/10.47852/bonviewJCCE2202192.

[22] Preethi, P., Mamatha, H.R.: Region-based convolutional neural network for segmenting text in epigraphical images. Artificial Intelligence and Applicatons. 1 (2), 119–127. https://doi.org/10.47852/bonviewAIA2202293.

[23] S. Saminu, et al., Applications of artificial intelligence in automatic detection of epileptic seizures using EEG signals: a review, Artif. Intell. Appl. 1 (1) (2023) 11–25, https://doi.org/10.47852/bonviewAIA2202297.

[24] L. Ma, et al., Apple grading method based on neural network with ordered partitions and evidential ensemble learning, CAAI Trans. Intell. Technol. 7 (4) (2022) 561–569, https://doi.org/10.1049/cit2.12140.

[25] B. Yang, et al., Enhancing direct-path relative transfer function using deep neural network for robust sound source localization, CAAI Trans. Intell. Technol. 7 (3) (2022) 446–454, https://doi.org/10.1049/cit2.12024.

[26] R. Rostamzadeh-Renani, D. J. Jasim, M. Baghoolizadeh, M. Rostamzadeh-Renani, H. T. Andani, S. Salahshour, S. Baghaei, Multi-objective optimization of rheological behavior of nanofluids containing CuO nanoparticles by NSGA II, MOPSO, and MOGWO evolutionary algorithms and group method of data handling artificial neural networks, Materials Today. Communications 38 (107709) (2024) 107709. https://doi.org/10.1016/j.mtcomm.2023.107709.

[27] X. Dai, H.T. Andani, A. Alizadeh, A.M. Abed, G.F. Smaisim, S.K. Hadrawi, M. Karimi, M. Shamsborhan, D. Toghraie, Using Gaussian Process Regression (GPR) models with the Matérn covariance function to predict the dynamic viscosity and torque of SiO2/Ethylene glycol nanofluid: a machine learning approach, Eng. Appl.

Artif. Intell. 122 (106107) (2023) 106107, https://doi.org/10.1016/j.engappai.2023.106107.
[28] B. Ruhani, M.T. Andani, A.M. Abed, N. Sina, G.F. Smaisim, S.K. Hadrawi, D. Toghraie, Statistical modeling and investigation of thermal characteristics of a new nanofluid containing cerium oxide powder, Heliyon 8 (11) (2022) e11373.
[29] B. Fan, et al., Intelligent vehicle lateral control based on radial basis function neural network sliding mode controller, CAAI Trans. Intell. Technol. 7 (3) (2022) 455–468, https://doi.org/10.1049/cit2.12075.
[30] Z. Chen, Research on internet security situation awareness prediction technology based on improved RBF neural network algorithm, J. Comput. Cogn. Eng. (2022), https://doi.org/10.47852/bonviewJCCE149145205514.